Synthesis of a Magneto-Rheological Vehicle Suspension System Built on the Variable Structure Control Approach

Leonardo Tavares Stutz

ltstutz@iprj.uerj.br
Polytechnic Institute – IPRJ
State University of Rio de Janeiro
Department of Mechanical Engineering
and Energy
28630-050 Nova Friburgo, RJ, Brazil

Fernando Alves Rochinha

faro@mecanica.ufrj.br
Federal University of Rio de Janeiro
Department of Mechanical Engineering
21941-914 Rio de Janeiro, RJ, Brazil

The synthesis of a magneto-rheological vehicle suspension system built on the variable structure control approach is considered in the present work. The suspension is synthesized in order to improve the ride comfort obtained by a standard passive suspension. Although a nominal half-vehicle model with rigid body is considered in the synthesis of the suspension, phenomenological models for the MR dampers and for the seat-driver subsystem, along with the flexibility of the vehicle body, are considered in the performance assessment. For comparison purposes, active and magneto-rheological suspensions built on the optimal control approach and an active suspension built on the variable structure control approach are also considered. The numerical results show that the proposed suspension outperforms the passive suspension and presents a performance comparable to that of the active ones when the vehicle body may be assumed as rigid. Besides, when its flexibility is an important issue, a great performance drop may be observed, depending on the road quality, the damper characteristics and the adopted control strategy.
Keywords: *magneto-rheological suspension, variable structure control, flexible half-vehicle model, seat-driver subsystem*

Introduction

A vehicle suspension system must fulfill several purposes, namely: support the vehicle weight; provide stability (handling) and directional control (road holding) during maneuvers and braking; and provide effective isolation of the vehicle body from road-induced disturbances (ride comfort) (Hrovat, 1997). Besides, the suspension system must also satisfy a design constraint related to the limited space available for its deflection. These different tasks, along with the spatial constraint, yield conflicting design trade-offs that give rise to great technological challenges.

In conventional suspension systems, composed of springs and dampers or shock absorbers, the characteristics of the suspension elements cannot be changed and, hence, conflicting trade-offs between different performance indices, such as ride comfort and road holding, are extremely difficult to be achieved (Sharp and Hassan, 1986). As a consequence, these passive suspensions are only effective in a limited range of the vehicle operation.

Much more flexible and, consequently, more effective systems can be obtained through the use of active suspensions (Hrovat, 1997; Shirahatt et al., 2008), in which externally powered forces are provided according to measured responses of the system and to some control strategy. Although active suspensions present great improvements on the performances obtained by conventional passive ones, they often require excessive power supply and sophisticated electronic devices. Besides, due to its complexity, an active suspension may not present the reliability of conventional passive systems.

In order to circumvent those technical difficulties, a lot of effort has been recently devoted to semi-active suspensions (Yokoyama, Hedrick and Toyama, 2001; Stutz and Rochinha, 2005; Nguyen and Choi, 2009). Basically, semi-active suspensions differ from the passive ones by the fact that their stiffness and/or damping properties can be actively changed according to some control strategy. The semi-active systems represent some of the most promising devices for practical applications in vibration isolation problems. This is due to their inherent stability and versatility, besides the relative simplicity and much lower power demand as compared with their active counterparts (Carlson and Spencer Jr., 1996).

The development of electro-rheological (ER) and magneto-rheological (MR) dampers increased the applicability of the semi-active suspensions. In these devices, the rheological properties (elasticity, plasticity and viscosity) of their fluids can be reversibly changed in the presence of electric and magnetic fields, respectively. Therefore, the semi-active dampers are only capable to dissipate energy from the system in a passive manner, but with a rate that may be actively controlled through the control of the electric or magnetic fields. Hence, the energy required to generate these appropriate fields is just the one required by the ER or MR dampers. This energy is considerably lower than that required by active devices, as, for instance, hydraulic actuators. However, due to the highly nonlinear dynamic behavior of these semi-active systems, one of the main challenges to their practical application is the development of appropriate control algorithms (Jansen and Dyke, 2000; Stutz and Rochinha, 2005). Several models have been proposed in order to model the dynamic behavior of the MR dampers. These include polynomial models (Choi, Lee and Park, 2001; Du, Sze and Lam, 2005), a neural network model (Chang and Zhou, 2002), phenomenological models built on the Bouc-Wen hysteretic model (Spencer Jr. et al., 1996), among others.

The variable structure control approach is known to be robust and even insensitive to some classes of system disturbances (Edwards and Spurgeon, 1998). Therefore, due to dynamic complexities, parameter uncertainties and varying operational conditions, always present in vehicle suspension problems, different active and semi-active suspensions built on the variable structure control approach have been proposed in the literature. In Yokoyama, Hedrick and Toyama (2001) the variable structure control was considered to synthesize a MR suspension system for a quarter-car model. In that paper, the control law was derived so that the dynamics of the system followed a desired one provided by a reference model. The research showed that the proposed suspension achieved satisfactory performance only in the low frequency range. In Stutz and Rochinha (2007) the same strategy was extended to a half vehicle model. Besides, a phenomenological model of the seat-driver subsystem and the modified Bouc-Wen model of the MR damper were also considered in the numerical assessment of the proposed suspension. The numerical results showed that the proposed suspension outperformed the standard passive one. In Liangbin and

Paper received 25 April 2011. Paper accepted 8 August 2011.
Technical Editor: Domingos Rade

Dayue (2004), a variable structure suspension system built only on the measured output was presented. A mathematical model of a ER damper was experimentally derived and it was considered in numerical simulations that showed the effectiveness of the suspension even in the presence of parameter uncertainties. In (Yoshimura et al., 2001; Sung et al., 2008), the effectiveness of vehicle suspensions systems built on the variable structure control were experimentally demonstrated.

In the present work, a MR suspension system is synthesized, built on the variable structure control approach with model tracking, which is a well known robust control approach (Edwards and Spurgeon, 1998). The main objective of the work is to synthesize a variable structure suspension system based on a simple nominal half vehicle model, since the variable structure control approach is supposed to deal with some unmodeled dynamics and parameters uncertainties, which are commonly present in a vehicle suspension design. A nominal half vehicle model with a rigid body is, therefore, assumed in the synthesis of the suspension. However, due to the semi-active nature of the MR dampers, with a highly hysteretic behavior, and due to the control structure interaction, the performance potentials of the system were numerically assessed considering a more practical situation, that is, taking into account the MR damper behavior, the flexibility of the vehicle body, and the seat-driver subsystem. Most papers in the literature do consider a vehicle with a rigid body in the synthesis of a vehicle suspension; however, some important issues that may considerably affect the performance of the suspensions, as for example the flexibility of the vehicle body, are not always considered.

Here, the MR suspension is synthesized considering a half-vehicle model with rigid body (Stutz, 2005). A reference model, based on a nominal vehicle model, and the optimal control approach are considered for specifying the desired dynamics for the vehicle body. Then, a variable structure control force is derived in order to compel the tracking error dynamics, between the state of the vehicle body and that of the reference model, to attain a sliding mode. Finally, due to the fact that the MR dampers only dissipate energy from the system, to induce the dampers to approximately reproduce the desired variable structure control force, the input voltages to their current drivers are derived according to the clipped-control algorithm (Jansen and Dyke, 2000).

Steady-state and transient performances of the proposed suspension are assessed through numerical analyses, where phenomenological models for the MR dampers and for the seat-driver subsystem, along with a half-vehicle model with flexible body, are taken into account. For comparison purposes, active and MR suspensions built on the optimal control approach and an active suspension built on the variable structure control approach were also considered in the numerical analysis.

Nominal Model: Half-Vehicle Model with Rigid Body

In the present work, a half-vehicle model with rigid body is considered for the synthesis of a magneto-rheological (MR) vehicle suspension system. In this model, depicted in Fig. 1, the vehicle body has mass m_1 and moment of inertia J with respect to its center of gravity G. The masses m_{2f} and m_{2r} are the effective ones of the front and rear suspensions, respectively. The suspensions are composed of springs k_{1f} and k_{1r}; conventional dampers d_{1f} and d_{1r}; and, in the case of active or semi-active suspensions, control elements which perform the control forces u_f and u_r. The stiffness and damping of the tyres are modeled by linear springs, k_{2f} and k_{2r}, and dampers, d_{2f} and d_{2r}, respectively.

The geometrical parameters a_1, a_2 and b_2 define the position of the points P_f and P_r, which are connection points between the front and rear suspensions and the vehicle body, respectively.

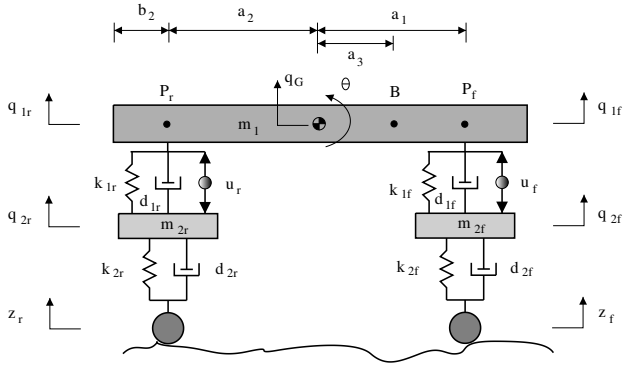

Figure 1. Half-vehicle model with rigid body.

The dynamic behavior of the half-vehicle model is given by:

$$\begin{aligned}
&m_1\ddot{q}_G + d_{1f}(\dot{q}_{1f} - \dot{q}_{2f}) + d_{1r}(\dot{q}_{1r} - \dot{q}_{2r}) \\
&\qquad + k_{1f}(q_{1f} - q_{2f}) + k_{1r}(q_{1r} - q_{2r}) = u_f + u_r; \\
&J\ddot{\theta} + a_1 d_{1f}(\dot{q}_{1f} - \dot{q}_{2f}) - a_2 d_{1r}(\dot{q}_{1r} - \dot{q}_{2r}) \\
&\qquad + a_1 k_{1f}(q_{1f} - q_{2f}) - a_2 k_{1r}(q_{1r} - q_{2r}) = a_1 u_f - a_2 u_r; \\
&m_{2f}\ddot{q}_{2f} + d_{2f}\dot{q}_{2f} + d_{1f}(\dot{q}_{2f} - \dot{q}_{1f}) \\
&\qquad + k_{2f} q_{2f} + k_{1f}(q_{2f} - q_{1f}) = -u_f + d_{2f}\dot{z}_f + k_{2f} z_f; \\
&m_{2r}\ddot{q}_{2r} + d_{2r}\dot{q}_{2r} + d_{1r}(\dot{q}_{2r} - \dot{q}_{1r}) + k_{2r} q_{2r} \\
&\qquad + k_{1r}(q_{2r} - q_{1r}) = -u_r + d_{2r}\dot{z}_r + k_{2r} z_r.
\end{aligned} \tag{1}$$

where $(\cdot)$ represents the differentiation with respect to time, q_G is the vertical displacement of the center of gravity G; θ is the angular displacement of the vehicle body; q_{1f} and q_{1r} are the vertical displacements of the connection points P_f and P_r, respectively; q_{2f} and q_{2r} are the displacements of the front and rear wheels; and z_f and z_r are front and rear disturbances due to the movement of the vehicle over an unevenness road.

Assuming that the vehicle body undergoes small rotations about its center of gravity G, one has the following approximations:

$$\begin{aligned}
q_{1f} &= q_G + a_1\theta; \\
q_{1r} &= q_G - a_2\theta.
\end{aligned} \tag{2}$$

Defining the generalized displacement vector

$$\mathbf{q} = [q_G \quad \theta \quad q_{2f} \quad q_{2r}]^T, \tag{3}$$

where T means transpose, the dynamic equations in (1) may be written in matrix form as

$$\mathbf{M}\ddot{\mathbf{q}} + \mathbf{D}\dot{\mathbf{q}} + \mathbf{K}\mathbf{q} = \mathbf{B}'\mathbf{u} + \mathbf{B}'_{f_z}\mathbf{f}_z, \tag{4}$$

where $\mathbf{M}$, $\mathbf{D}$ and $\mathbf{K}$ are, respectively, the mass, damping and stiffness matrices of the system; $\mathbf{B}'$ and $\mathbf{B}'_{f_z}$ are input matrices related to the control action $\mathbf{u}$ and the road-induced disturbance $\mathbf{f}_z$, which are defined as

$$\mathbf{u} = \begin{bmatrix} u_f \\ u_r \end{bmatrix} \qquad \text{and} \qquad \mathbf{f}_z = \begin{bmatrix} d_{2f}\dot{z}_f + k_{2f} z_f \\ d_{2r}\dot{z}_r + k_{2r} z_r \end{bmatrix}. \tag{5}$$

Therefore, considering Eqs. (3) and (4) and defining the state vector

$$\mathbf{x} = \begin{bmatrix} \mathbf{q} \\ \dot{\mathbf{q}} \end{bmatrix}, \tag{6}$$

the dynamics of the system may be described by the state-space equation

$$\dot{\mathbf{x}} = \mathbf{A}\mathbf{x} + \mathbf{B}\mathbf{u} + \mathbf{B}_{fz}\mathbf{f}_z. \tag{7}$$

It is worth emphasizing that, in the present work, the state vector $\mathbf{x}$, defined in Eq. (6), is assumed to be known. Hence, the state components are supposed to be directly measured or derived from other measured signals.

Magneto-Rheological Variable Structure Control (MR-VSC) Suspension System

The MR-VSC suspension was synthesized as follows. A reference model was considered for specifying the desired dynamics for the vehicle body. Then, a variable structure control force was derived in order to force the tracking error dynamics, between the state vector of the vehicle body and the corresponding one of the reference model, to attain a sliding mode (Yokoyama, Hedrick and Toyama, 2001). This force was taken as the desired one for the MR dampers. Finally, the clipped-control approach (Jansen and Dyke, 2000) was considered for determining an input voltage to the current drivers of the dampers such that the generated forces approximately reproduce the desired ones.

Considering the first two equations in (1) and defining the state vector

$$\mathbf{x}_b = [q_G \quad \theta \quad \dot{q}_G \quad \dot{\theta}]^T, \tag{8}$$

the actual dynamic behavior of the vehicle body may be written in a general state-space form as

$$\dot{\mathbf{x}}_b = \mathbf{A}_b\mathbf{x}_b + \mathbf{B}_b\left(\mathbf{u} + \mathbf{f}_2 + \mathbf{f}_\phi + \mathbf{f}_p\right), \tag{9}$$

where $\mathbf{u}$ is the control action defined in (5); $\mathbf{f}_2$ is a known input signal defined from nominal parameters of the suspensions and the wheel dynamics, which is considered as known, viz.

$$\mathbf{f}_2 = \begin{bmatrix} d_{1f}\dot{q}_{2f} + k_{1f}q_{2f} \\ d_{1r}\dot{q}_{2r} + k_{1r}q_{2r} \end{bmatrix}; \tag{10}$$

the unknown signal $\mathbf{f}_\phi$ accounts for disturbances resulting from unmodeled dynamics, as, for instance, the ones resulting from the flexibility of the vehicle body; and, finally, the unknown signal $\mathbf{f}_p$ accounts for parameter uncertainties and it is given by

$$\mathbf{f}_p = \begin{bmatrix} -\Delta d_{1f}(\dot{q}_{1f} - \dot{q}_{2f}) - \Delta k_{1f}(q_{1f} - q_{2f}) - \left(\dfrac{a_2\Delta m_1\ddot{q}_G + \Delta J\ddot{\theta}}{a_1 + a_2}\right) \\ -\Delta d_{1r}(\dot{q}_{1r} - \dot{q}_{2r}) - \Delta k_{1r}(q_{1r} - q_{2r}) - \left(\dfrac{a_1\Delta m_1\ddot{q}_G - \Delta J\ddot{\theta}}{a_1 + a_2}\right) \end{bmatrix}, \tag{11}$$

where $\Delta(\cdot)$ represents the uncertainty on the nominal parameter $(\cdot)$.

Synthesis of the reference model

In order to specify the desired dynamics for the vehicle body, the reference model depicted in Fig. 2 was adopted. All parameters in this model are counterparts of those in the nominal vehicle model depicted in Fig. 1. One should note, from Fig. 2, that the reference model dynamics does depend on the actual dynamics of the wheels, that is, it depends on $q_{2f}, q_{2r}, \dot{q}_{2f}$ and $\dot{q}_{2r}$.

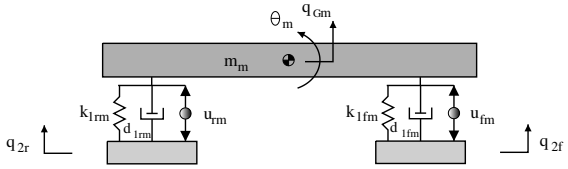

Figure 2. Reference model for the vehicle body.

The dynamics of the reference model vehicle body is given by

$$\dot{\mathbf{x}}_{bm} = \mathbf{A}_{bm}\mathbf{x}_{bm} + \mathbf{B}_{bm}\left(\mathbf{u}_m + \mathbf{f}_{2m}\right), \tag{12}$$

where $\mathbf{u}_m$ is the control force vector; the state vector $\mathbf{x}_{bm}$ and the input signal $\mathbf{f}_{2m}$ are the reference model counterparts of those signals in Eqs. (8) and (10) for the vehicle body, viz.

$$\mathbf{x}_{bm} = [q_{Gm} \quad \theta_m \quad \dot{q}_{Gm} \quad \dot{\theta}_m]^T, \tag{13}$$

and

$$\mathbf{f}_{2m} = \begin{bmatrix} d_{1fm}\dot{q}_{2f} + k_{1fm}q_{2f} \\ d_{1rm}\dot{q}_{2r} + k_{1rm}q_{2r} \end{bmatrix}. \tag{14}$$

It is worth noting that, in the particular case when the reference model parameters are adopted as the corresponding ones of the nominal vehicle model, one has

$$\mathbf{f}_{2m} = \mathbf{f}_2. \tag{15}$$

Therefore, in order to the reference model dynamics, given by Eq. (12), be the desired one for the vehicle body, the control force $\mathbf{u}_m$ should be properly determined.

In the present work, the aim of the proposed suspension is to improve the ride comfort obtained by standard passive suspension systems and, for the purpose of establishing its performance potentials, the root mean square value of the vertical and pitch accelerations are considered throughout the paper as an adequate measure of ride quality. The smaller the rms value of the accelerations, the greater the subjective ride comfort experienced (Smith, McGehee and Healey, 1978).

Here, the optimal control approach was considered for determining the dynamics of the reference model. The following performance index, that trades off ride comfort and suspension deflections, while maintaining constraints on the control effort, was adopted:

$$\begin{aligned} J_m = \lim_{T\to\infty}\frac{1}{T}\int_0^T \Big\{ & r_1(\ddot{q}_{Gm})^2 + r_2(\ddot{\theta}_m)^2 \\ & + r_3\left[(q_{1fm} - q_{2f})^2 + (q_{1rm} - q_{2r})^2\right] \\ & + r_4(u_{fm}^2 + u_{rm}^2)\Big\}\, dt, \end{aligned} \tag{16}$$

where r_1, r_2, r_3 and r_4 are weighting coefficients. The coefficients r_1 and r_2 weight the ride comfort, which are related to the mean square value of the vertical and pitch accelerations, respectively. The smaller the rms value of the accelerations, the greater the subjective ride comfort (Smith, McGehee and Healey, 1978; Hrovat, 1997). The coefficient r_3 weights the mean square value of the suspension deflections,

which takes into account the limited stroke capability of the suspensions, and the coefficient r_4 weights the mean square value of the control efforts. It is worth noting that the performance index in Eq. (16) and, consequently, the dynamics of the reference model do not explicitly depend on the road disturbances z_f and z_r.

The desired dynamics for the vehicle body is, therefore, defined as follows: considering the reference model described by Eq. (12), the control action $\mathbf{u}_m$ is determined such that the performance index given by Eq. (16), which reflects the desired dynamics, is minimized.

The performance index (16) may be expressed as a quadratic form of the state vector $\mathbf{x}_{bm}$ and the control action $\mathbf{u}_m$ as

$$J_m = \lim_{T\to\infty} \frac{1}{T} \int_0^T \left\{ \mathbf{x}_{bm}^T \mathbf{Q}_m \mathbf{x}_{bm} + 2\mathbf{x}_{bm}^T \mathbf{N}_m \mathbf{u}_m + \mathbf{u}_m^T \mathbf{R}_m \mathbf{u}_m \right\} dt. \tag{17}$$

As it can be shown (Anderson and Moore, 1990), the control force that minimizes the performance index (17), under the dynamic constraint given by Eq. (12), is given by

$$\mathbf{u}_m = -\mathbf{G}_m \mathbf{x}_{bm}, \tag{18}$$

with the optimal gain matrix $\mathbf{G}_m$ given by

$$\mathbf{G}_m = \mathbf{R}_m^{-1} \left(\mathbf{N}_m^T + \mathbf{B}_{bm}^T \mathbf{P}_m \right), \tag{19}$$

where $\mathbf{P}_m$ is the symmetric positive definite matrix solution of the algebraic Riccati equation

$$\mathbf{P}_m \bar{\mathbf{A}}_m + \bar{\mathbf{A}}_m^T \mathbf{P}_m - \mathbf{P}_m \mathbf{B}_{bm} \mathbf{R}_m^{-1} \mathbf{B}_{bm}^T \mathbf{P}_m + \bar{\mathbf{Q}}_m = \mathbf{0}, \tag{20}$$

where $\bar{\mathbf{A}}_m$ and $\bar{\mathbf{Q}}_m$ are defined as:

$$\begin{aligned} \bar{\mathbf{A}}_m &= \left(\mathbf{A}_{bm} - \mathbf{B}_{bm} \mathbf{R}_m^{-1} \mathbf{N}_m^T \right); \\ \bar{\mathbf{Q}}_m &= \mathbf{Q}_m - \mathbf{N}_m \mathbf{R}_m^{-1} \mathbf{N}_m^T. \end{aligned} \tag{21}$$

Synthesis of the variable structure control force

Defining the tracking error vector as the difference between the response of the vehicle body $\mathbf{x}_b$ and that of the reference model $\mathbf{x}_{bm}$, viz.

$$\mathbf{e} = \mathbf{x}_b - \mathbf{x}_{bm}, \tag{22}$$

and considering Eqs. (9) and (12), the error dynamics is governed by

$$\dot{\mathbf{e}} = \mathbf{A}_{bm}\mathbf{e} + \mathbf{B}_b \mathbf{u} + \mathbf{f}_k + \mathbf{f}_m, \tag{23}$$

where the signals $\mathbf{f}_k$ and $\mathbf{f}_m$ are defined as:

$$\begin{aligned} \mathbf{f}_k &= \left[\mathbf{A}_b - \mathbf{A}_{bm} \right] \mathbf{x}_b + \mathbf{B}_b \mathbf{f}_2 - \mathbf{B}_{bm} \left(\mathbf{u}_m + \mathbf{f}_{2m} \right); \\ \mathbf{f}_m &= \mathbf{B}_b \left(\mathbf{f}_p + \mathbf{f}_\phi \right). \end{aligned} \tag{24}$$

It is worth noting that $\mathbf{f}_k$ is a known signal, since it is composed of system nominal matrices, reference model matrices and other known signals. The signal $\mathbf{f}_m$, on the other hand, represents an unknown matched disturbance, since it is described as the product of the input matrix $\mathbf{B}_b$ and other signals (Edwards and Spurgeon, 1998). According to Eq. (24), the disturbance $\mathbf{f}_m$ is associated with unmodeled dynamics, through $\mathbf{f}_\phi$, and parameter uncertainties, through $\mathbf{f}_p$, which is defined in Eq. (11).

In the particular case where the reference model parameters are adopted as the nominal parameters of the vehicle, the signal $\mathbf{f}_k$ is given as

$$\mathbf{f}_k = -\mathbf{B}_b \mathbf{u}_m. \tag{25}$$

One may define a sliding surface $\mathscr{S}$ in the error space as

$$\mathscr{S} = \{ \mathbf{e} \in \mathbf{R}^4 \mid \mathbf{s} = \mathbf{0} \}, \tag{26}$$

where $\mathbf{s}$ is an error-dependent switching function defined as

$$\mathbf{s} = \mathbf{S}\mathbf{e}, \tag{27}$$

where $\mathbf{S} \in I\!R^{2\times 4}$ is a design matrix of full rank which specifies the sliding surface $\mathscr{S}$. The matrix $\mathbf{S}$ may be partitioned as

$$\mathbf{S} = \begin{bmatrix} \mathbf{S}_1 & \mathbf{S}_2 \end{bmatrix}, \tag{28}$$

where $\mathbf{S}_1 \in I\!R^{2\times 2}$ and $\mathbf{S}_2 \in I\!R^{2\times 2}$. For the existence and uniqueness of the sliding mode, a necessary condition is that matrix $\mathbf{S}_2$ be nonsingular (Edwards and Spurgeon, 1998).

The error dynamics, when constrained to the sliding surface $\mathscr{S}$, is described as a sliding mode and, according to Eqs. (26) and (27), one has

$$\mathbf{S}\mathbf{e} = 0. \tag{29}$$

Differentiating Eq. (27) and considering Eqs. (23) and (29) yields

$$\mathbf{S} \left(\mathbf{A}_{bm}\mathbf{e} + \mathbf{B}_b \mathbf{u} + \mathbf{f}_k + \mathbf{f}_m \right) = 0. \tag{30}$$

Assuming the matrix $\mathbf{S}\mathbf{B}_b$ is chosen to be nonsingular, an unique control input, named equivalent control, may be obtained from the algebraic equation in (30), viz.

$$\mathbf{u}_{eq} = -\left(\mathbf{S}\mathbf{B}_b \right)^{-1} \mathbf{S} \left[\mathbf{A}_{bm}\mathbf{e} + \mathbf{f}_k + \mathbf{f}_m \right]. \tag{31}$$

The equivalent control represents a sufficient control input to maintain the dynamics of the system in sliding mode (Edwards and Spurgeon, 1998).

Substituting the equivalent control, given by Eq. (31), in Eq. (23) and considering the fact that the signals $\mathbf{f}_k$ and $\mathbf{f}_m$ are matched, one has the error dynamics during the sliding mode

$$\dot{\mathbf{e}} = \left[\mathbf{I} - \mathbf{B}_b \left(\mathbf{S}\mathbf{B}_b \right)^{-1} \mathbf{S} \right] \mathbf{A}_{bm}\mathbf{e}, \tag{32}$$

where $\mathbf{I}$ is the identity matrix.

Therefore, according to Eq. (32), the error dynamics is independent of the control input $\mathbf{u}$ and it is invariant with respect to the matched disturbance $\mathbf{f}_m$, which is related to unmodeled dynamics and parameters uncertainties. Hence, a reference model and a sliding surface matrix may be properly synthesized in such a way that the error dynamics asymptotically goes to zero, despite the presence of matched unmodeled dynamics and parameter uncertainties.

It can be seen (Edwards and Spurgeon, 1998) that the following control law gives sufficient conditions for inducing and maintaining the error dynamics in sliding mode

$$\mathbf{u} = \mathbf{u}_l + \mathbf{u}_n, \tag{33}$$

where $\mathbf{u}_l$ and $\mathbf{u}_n$ are, respectively, the linear and nonlinear parts of the control law, which are given as follows.

$$\mathbf{u}_l = -\left(\mathbf{S}\mathbf{B}_b \right)^{-1} \mathbf{S} \left[\mathbf{A}_{bm}\mathbf{e} + \mathbf{f}_k \right] + \left(\mathbf{S}\mathbf{B}_b \right)^{-1} \Phi \mathbf{s}, \tag{34}$$

where $\Phi \in I\!R^{2\times 2}$ is an arbitrary matrix whose eigenvalues have negative real parts;

$$\mathbf{u}_n = -\rho\left(\mathbf{S}\mathbf{B}_b\right)^{-1}\frac{\mathbf{P}_2\mathbf{s}}{\|\mathbf{P}_2\mathbf{s}\|+\delta}\,, \quad \text{for} \quad \mathbf{s}\neq 0, \tag{35}$$

where δ is an arbitrary positive scalar defined in order to minimize the chattering phenomenon (Edwards and Spurgeon, 1998), inherent in a variable structure control action, $\mathbf{P}_2$ is a symmetric positive definite matrix satisfying the Lyapunov equation

$$\mathbf{P}_2\Phi + \Phi^T\mathbf{P}_2 = -\mathbf{I}, \tag{36}$$

with $\mathbf{I}$ being the identity matrix, and ρ a modulation function, which must satisfy the inequality

$$\rho \geq \|\mathbf{S}_2\|\,\|\bar{\mathbf{f}}_m\| + \eta, \tag{37}$$

where $\|\cdot\|$ is the norm of $(\cdot)$, η is an arbitrary positive constant, $\mathbf{S}_2$ is given in Eq. (28) and $\bar{\mathbf{f}}_m$ is the projection of $\mathbf{f}_m$ into the range space of $\mathbf{B}_b$.

A modulation function satisfying the inequality (37) ensures a global asymptotic stability for the error dynamics (Edwards and Spurgeon, 1998; Stutz and Rochinha, 2005); however, the signal $\mathbf{f}_m$ is unknown. A constant modulation function may also be chosen, although, in this case, only a local stability can be proven.

It must be emphasized here that the focus of the present research is to assess the performance potentials of the proposed MR-VSC suspension system for different types of road conditions and in the presence of unmodeled dynamics. Therefore, as usual in this case, the assumption of the entire state vector is plausible (Hrovat, 1997; Shirahatt et al., 2008). In practice, the suspension strokes, the velocities of the wheels and velocities of the connection points P_f and P_r are easily accessible, so that the applicability of the MR-VSC suspension, as presented here, relies on the estimation of the entire state vector of the system through a suitable state observer (Hrovat, 1997; Sung et al., 2008), yielding, of course, some drop in the suspension performance.

The clipped-control algorithm

Due to their semi-active nature, the MR dampers are not able to perform an active control force, as the variable structure control one given by Eqs. (33)-(35). Besides, only the input voltages to the current drivers of the MR dampers can be directly controlled. Therefore, to induce the MR dampers to approximately generate the desired control action, the clipped-control approach (Jansen and Dyke, 2000) was considered. In this approach, the input voltage vector, composed of the input voltages V_f and V_r to the front and rear dampers, respectively, is given by

$$\mathbf{V} = V_{max}\mathrm{H}\left[(\mathbf{u}-\mathbf{u}_{MR})^T\mathbf{u}_{MR}\right], \tag{38}$$

where V_{max} is the maximum applied voltage, $\mathbf{u}_{MR}$ is the force actually provided by the MR dampers, $\mathbf{u}$ is the desired control force and $\mathrm{H}(\cdot)$ is the unit step function. Therefore, according to Eq. (38), the clipped-control strategy only applies the extreme voltages, 0 or V_{max}, to the current driver of the dampers.

Therefore, to implement the MR-VSC suspension, the clipped-control algorithm was adopted, with the desired control force given by Eqs. (33)-(35). The clipped-control approach was adopted due to its simplicity and to the fact that it has succeeded in practical applications of MR dampers in control problems (Jansen and Dyke, 2000). It would certainly be more beneficial to have a continuous voltage applied to the damper. However, as will be seen, the dynamics of the MR dampers is highly nonlinear and, as a consequence, it is not a simple task to derive a model that accounts for its dynamics and directly relates the desired control force with the required voltage to the dampers. Figure 3 illustrates the clipped-control algorithm when applied to one of the MR dampers.

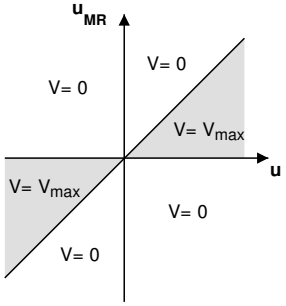

Figure 3. Clipped-control algorithm.

Magneto-Rheological Linear Quadratic Gaussian (MR-LQG) Suspension System

In the present work, a MR vehicle suspension system based on the linear quadratic gaussian (LQG) optimal control approach is also considered for comparison purposes.

When considering ride comfort, the road-induced disturbances are the most important ones in the performance assessment of vehicle suspension systems (Hrovat, 1997). Therefore, in order to synthesize the MR-LQG suspension, a model must be first considered for deriving the actual road-induced disturbances from white noise processes, as required by the LQG control theory.

Disturbances induced by an unevenness road

In this subsection, a mathematical model of the disturbances induced by the movement of the vehicle with a constant velocity on an unevenness road is considered.

The road disturbance vector $\mathbf{z}$ is defined as

$$\mathbf{z} = \begin{bmatrix} z_f \\ z_r \end{bmatrix} \tag{39}$$

and its components are modeled as stationary gaussian processes with spectral density

$$S_z(\omega) = \frac{\sigma^2}{\pi}\frac{av}{(av)^2+\omega^2}\,, \tag{40}$$

where σ^2 denotes the variance of the road irregularities, v is the vehicle velocity and a is a coefficient dependent on the type of the road surface (Hać, 1985).

Considering the spectral density in (40), the road disturbance vector $\mathbf{z}$ may be obtained from white noise processes according to the differential equation

$$\dot{\mathbf{z}} = \mathbf{A}_z\mathbf{z} + \mathbf{I}\xi, \tag{41}$$

where $\mathbf{I}$ is the identity matrix,

$$\mathbf{A}_z = \begin{bmatrix} -av & 0 \\ 0 & -av \end{bmatrix} \tag{42}$$

and

$$\xi = \begin{bmatrix} \xi_f \\ \xi_r \end{bmatrix}, \tag{43}$$

where the signals ξ_f and ξ_r are zero mean white noise processes with covariance functions

$$\begin{aligned} E\left[\xi_f(t)\xi_f(t+\tau)\right] &= 2\sigma^2 av\delta(\tau); \\ E\left[\xi_r(t)\xi_r(t+\tau)\right] &= 2\sigma^2 av\delta(\tau), \end{aligned} \tag{44}$$

where $E[\cdot]$ is the expected value of $(\cdot)$, τ is an arbitrary time delay and δ is the Dirac's delta function. However, since in a half-vehicle model, the road disturbance under the rear wheel is the time-delayed disturbance under the front wheel, one has

$$\xi_r(t) = \xi_f\left(t - \frac{a_1 + a_2}{v}\right), \tag{45}$$

where $(a_1 + a_2)$ is the distance between the centers of the rear and front wheels (see Fig. 1).

Therefore, according to Eq. (41), the road disturbance vector $\mathbf{z}$, induced by the movement of the vehicle on an unevenness road, is given by the output of a linear system to the input ξ, whose components are white noise processes.

Synthesis of the linear quadratic gaussian control force

The following performance index, which trades off ride comfort and tyre deflections, while maintaining constraints on suspension deflections and control efforts, was adopted for the synthesis of the MR-LQG suspension system.

$$\begin{aligned} J = \lim_{T\to\infty} \frac{1}{T}\int_0^T \Big\{ & \rho_1 (\ddot{q}_G)^2 + \rho_2(\ddot{\theta})^2 \\ & + \rho_3\left[(q_{1f} - q_{2f})^2 + (q_{1r} - q_{2r})^2\right] \\ & + \rho_4\left[(q_{2f} - z_f)^2 + (q_{2r} - z_r)^2\right] + \rho_5(u_f^2 + u_r^2)\Big\} dt, \end{aligned} \tag{46}$$

where ρ_1, ρ_2, ρ_3, ρ_4 and ρ_5 are weighting coefficients.

It must be emphasized that the MR-LQG suspension is only considered for comparison purposes; therefore, the not so practical assumption of the knowledge of the road disturbances, z_f and z_r, is adopted here. The aim is to obtain a suspension system with better performance indices to be compared with the proposed semi-active MR-VSC suspension. A drop in the performance of these suspensions would be observed if a cost function similar to that in Eq. (16) was adopted, that is, if the road disturbances were not known. In this case, a sub-optimal performance would be obtained. Although the knowledge of the road disturbances is not straightforward, there are works in the literature where the prediction of these disturbances is considered in the design of vehicle suspensions (Roh and Park, 1999; Marzbanrad et al., 2002).

Defining the augmented state vector

$$\mathbf{x}_a = \begin{bmatrix} \mathbf{x} \\ \mathbf{z} \end{bmatrix} \tag{47}$$

and considering Eqs. (7) and (41), the dynamics of the vehicle may be rewritten as

$$\dot{\mathbf{x}}_a = \mathbf{A}_a\mathbf{x}_a + \mathbf{B}_a\mathbf{u} + \mathbf{B}_{a\xi}\xi, \tag{48}$$

where $\mathbf{u}$ is the control action and ξ is a vector composed by white noise processes, as defined in Eq. (43). Therefore, the performance index (46) may be expressed as a quadratic form of the augmented state vector $\mathbf{x}_a$ and the control action $\mathbf{u}$ as

$$J = \lim_{T\to\infty} \frac{1}{T}\int_0^T \left[\mathbf{x}_a{}^T\mathbf{Q}\mathbf{x}_a + 2\mathbf{x}_a^T\mathbf{N}\mathbf{u} + \mathbf{u}^T\mathbf{R}\mathbf{u}\right] dt. \tag{49}$$

Following a procedure similar to that for the reference model definition, an optimal control action, which minimizes the performance index (49) under the dynamic constraint given by Eq. (48), may be obtained as

$$\mathbf{u} = -\mathbf{G}_a\mathbf{x}_a, \tag{50}$$

where $\mathbf{G}_a$ is the optimal control gain.

Once again, to induce the MR dampers to approximately generate the desired optimal control force, given by Eq. (50), the input voltages to their current drivers are given by Eq. (38).

Numerical Analysis

In order to assess the performance of the MR suspensions with respect to ride comfort, numerical analysis considering a half-vehicle model were carried out. Although this model largely simplifies the actual structure, it includes the most fundamental characteristics of the system behavior.

Table 1 gives the nominal parameters of the vehicle model with rigid body and a standard passive suspension. These parameters were extracted from Hać, Youn and Chen (1996a) and they correspond to the ones of a mid-size vehicle.

Table 1. Nominal parameters of the half-vehicle model.

m_1	705 kg	J	945 kgm^2
m_{2f}	50 kg	m_{2r}	50 kg
d_{1f}	1560 Ns/m	d_{1r}	1309 Ns/m
k_{1f}	24 kN/m	k_{1r}	16.8 kN/m
d_{2f}	0 Ns/m	d_{2r}	0 Ns/m
k_{2f}	250 kN/m	k_{2r}	250 kN/m
a_1	1.30 m	a_2	1.22 m
a_3	0.46 m	b_2	1.06 m

Phenomenological models for the MR dampers and seat-driver subsystem were also considered for performance assessment. It is worth emphasizing that these models were not considered in the synthesis of the suspensions and, therefore, they represent sources of unmodeled dynamics.

Magneto-rheological damper

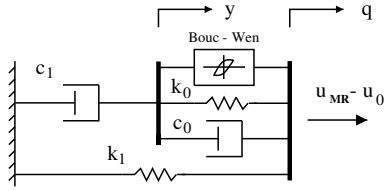

Figure 4. The modified Bouc-Wen model of the MR damper.

In order to model the nonlinear behavior of the MR damper, the modified Bouc-Wen model, depicted in Fig. 4, is adopted in this

work. This model is a phenomenological one composed of mechanical springs and dampers, along with a hysteresis element. The modified Bouc-Wen model has been shown to accurately predict the nonlinear behavior of prototype MR dampers over a wide range of operating conditions (Spencer Jr. et al., 1996).

In the modified Bouc-Wen model, the reaction force of the MR damper is given by

$$u_{MR} = c_1\dot{y} + k_1 q + u_0, \tag{51}$$

where the velocity $\dot{y}$ is given by

$$\dot{y} = \frac{1}{(c_0 + c_1)}[\alpha h + c_0\dot{q} + k_0(q - y)], \tag{52}$$

where h is the hysteretic displacement, whose evolution equation is

$$\dot{h} = -\gamma|\dot{q} - \dot{y}|\, h\, |h|^{n-1} - \beta(\dot{q} - \dot{y})|h|^n + \mathscr{A}(\dot{q} - \dot{y}), \tag{53}$$

with the parameters γ, β, $\mathscr{A}$ and n controlling the shape of the hysteresis loop.

Since, in a MR damper, the rheological properties of its fluid may be reversibly changed by exposing it to a controlled magnetic field, some parameters of the model are assumed to be dependent on the voltage V applied to the current driver as follows:

$$\begin{aligned} c_1(\mathscr{V}) &= c_{1a} + c_{1b}\mathscr{V}; \\ c_0(\mathscr{V}) &= c_{0a} + c_{0b}\mathscr{V}; \\ \alpha(\mathscr{V}) &= \alpha_a + \alpha_b\mathscr{V}; \end{aligned} \tag{54}$$

where the internal variable $\mathscr{V}$ is the output of the first order filter that accounts for the dynamics involved in reaching the rheological equilibrium (Spencer Jr. et al., 1996), viz.

$$\tau_f\dot{\mathscr{V}} + \mathscr{V} = V, \tag{55}$$

with τ_f being the time constant of the filter and V the voltage applied to the current driver.

The parameters of the modified Bouc-Wen model for the MR dampers were adopted according to the ones experimentally determined in Lai and Liao (2002) and are given in Table 2. With the aim at obtaining force intensities adequate to the present vehicle suspension problem, the forces obtained by the MR damper model with the parameters given in Table 2 were scaled by a factor of 0.2. It is worth noting that this procedure does preserve the hysteretic behavior of the MR dampers.

Table 2. Parameters of the MR damper model.

c_{1a}	14649 Ns/m	c_{0a}	784 Ns/m
c_{1b}	34622 Ns/(Vm)	c_{0b}	1803 Ns/(Vm)
k_1	840 N/m	k_0	3610 N/m
α_a	12441 N/m	β	2059020 m^{-2}
α_b	38430 N/(Vm)	γ	136320 m^{-2}
$\mathscr{A}$	58 N/m	n	2
u_0	20.6 N	τ_f	1/190 s

In order to illustrate the nonlinear behavior of the adopted model for the MR dampers, Fig. 5 presents the force-velocity curves obtained for different levels of applied voltage and for a sinusoidal displacement, with amplitude of 10 mm and frequency of 2 Hz, imposed at one end of the damper. This nonlinear dynamic behavior, inherent in the MR dampers, represents one of the main challenges to their practical application. The synthesis of a control algorithm that directly determines the required voltage to be applied to the dampers as a function of the damper parameters and of the damper dynamics is a very difficult task. Hence, in this work, the clipped-control approach given in Eq. (38) is adopted due to its simplicity.

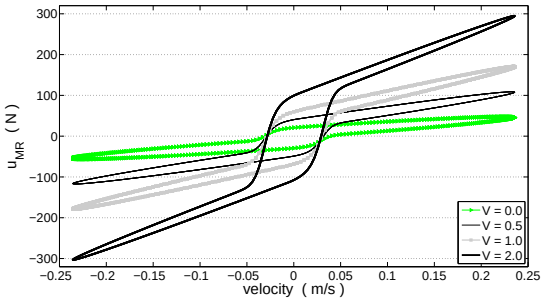

Figure 5. Force-velocity curves of the MR damper for different levels of applied voltage.

The MR suspensions considered in the present work were obtained just taking the standard passive dampers off and making the MR dampers as the control elements (see Fig. 1). The input voltages to the current driver of the dampers were selected according to the clipped-control algorithm with the maximum voltage $V_{max} = 2$ V, which is the value that yields a saturation of the magnetic field.

Seat-driver subsystem

A phenomenological model of the seat-driver subsystem, depicted in Fig. 6, will be considered for performance assessment. The seat is modeled by the spring k_{d1} and the damper d_{d1}. The driver, on the other hand, is modeled by a two degrees of freedom system composed of masses m_{d1}, m_{d2} and m_{d3}; springs k_{d2} and k_{d3}; and dampers d_{d2} and d_{d3}. With appropriated parameters, the present driver model presents an apparent mass similar to that of a seated human body exposed to vertical vibrations (Wei and Griffin, 1998a). The point C represents the driver position and the point B, located at a distance a_3 from the center of gravity of the vehicle body (see Fig. 1), is the connection point between the vehicle body and the seat-driver subsystem.

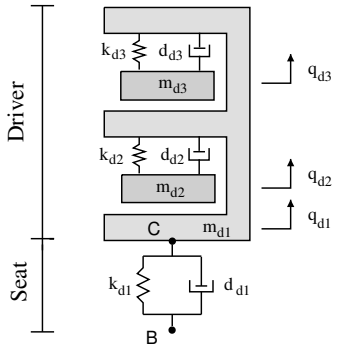

Figure 6. Phenomenological model of the seat-driver subsystem.

Table 3. Parameters of the seat-driver subsystem model.

m_{d1}	6.7 kg	k_{d1}	50210 N/m	d_{d1}	276 Ns/m
m_{d2}	33.4 kg	k_{d2}	35776 N/m	d_{d2}	761 Ns/m
m_{d3}	10.7 kg	k_{d3}	38374 N/m	d_{d3}	458 Ns/m

Considering the model depicted in Fig. 6, the dynamic behavior of the seat-driver subsystem is given by:

$$\begin{aligned} &m_{d1}\ddot{q}_{d1} + d_{d1}\dot{q}_{d1} + d_{d2}(\dot{q}_{d1} - \dot{q}_{d2}) \\ &\quad + d_{d3}(\dot{q}_{d1} - \dot{q}_{d3}) + k_{d1}q_{d1} + k_{d2}(q_{d1} - q_{d2}) \\ &\quad + k_{d3}(q_{d1} - q_{d3}) = d_{d1}\dot{q}_B + k_{d1}q_B; \\ &m_{d2}\ddot{q}_{d2} + d_{d2}(\dot{q}_{d2} - \dot{q}_{d1}) + k_{d2}(q_{d2} - q_{d1}) = 0; \\ &m_{d3}\ddot{q}_{d3} + d_{d3}(\dot{q}_{d3} - \dot{q}_{d1}) + k_{d3}(q_{d3} - q_{d1}) = 0. \end{aligned} \tag{56}$$

The parameters of the seat-driver subsystem model are given in Table 3. The parameters associated with the driver model was obtained from (Wei and Griffin, 1998a) and those associated with the seat model, on the other hand, were obtained from (Wei and Griffin, 1998b).

Synthesis of the suspensions

The MR-VSC suspension was obtained as follows. First, the parameters of the reference model were adopted as the ones of the nominal vehicle model. Then, in order to determine suitable weighting coefficients for the functional in Eq. (16), it was arbitrarily chosen $r_1 = 1$, $r_2 = 2$ and $r_4 = 10^{-6}$ and steady-state performance indices for the reference model were determined as a function of the weighting r_3. Figure 7 depicts the acceleration of point B and the front and rear tyre deflections, relative to the corresponding indices obtained for the passive suspension, as a function of the weighting coefficient r_3 and considering the disturbance induced by the movement of the vehicle at 20 m/s on a paved road (see Fig. 8).

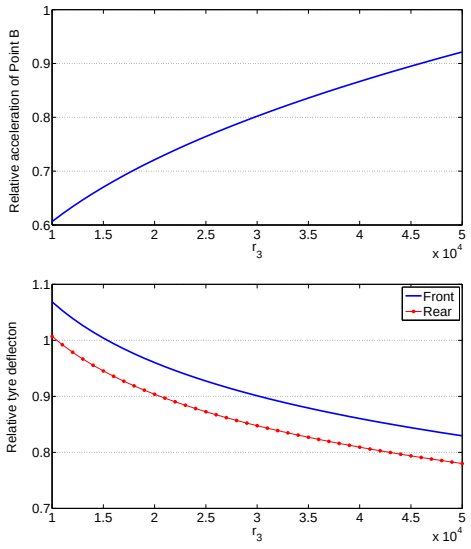

Figure 7. Relative performance of the reference model as a function of the weighting r_3.

Based on the indices depicted in Fig. 7, the value $r_3 = 2.35 \cdot 10^4$ was chosen, since this weighting yielded a rms value of 0.75 for the relative acceleration at point B while maintained the tyre deflections in acceptable values. In order to enable a fair comparison, the weighting coefficients associated with the MR-LQG suspension were determined in the same way, with the aim at obtaining the same improvement on ride comfort, relative to the passive suspension, for the same road condition.

The sliding surface $\mathscr{S}$ was defined adopting $\mathbf{S}_1$ and $\mathbf{S}_2$ as identity matrices. The stable matrix $\mathbf{\Phi}$ of the control law in Eq. (34) was adopted as minus the identity matrix, which resulted, from Eq. (36), in $\mathbf{P}_2 = 0.5\mathbf{I}$. The modulation function was adopted as $\rho = 3$ and, for reducing the chattering phenomenon, $\delta = 10^{-3}$. Finally, the input voltages to the MR dampers were determined according to Eq. (38), with the desired control law given by Eqs. (33)-(35).

The MR-LQG suspension was obtained considering the weighting coefficients $\rho_1 = 1$, $\rho_2 = 2$, $\rho_3 = 2 \cdot 10^3$, $\rho_4 = 2.5 \cdot 10^4$ and $\rho_5 = 10^{-6}$. The input voltages were selected according to Eq. (38) with the desired control force given by Eq. (50). It must be emphasized here that the implementation of the MR-LQG suspension, according to Eqs. (50) and (47), requires the knowledge of the road induced disturbances z_f and z_r.

For comparison purposes, active suspensions capable of integrally providing the control forces given by Eqs. (33) and (50) were also considered. These suspensions were named VSC and LQG, respectively. It is worth noting that these are ideal suspensions, since the dynamics of their actuators were not taken into account. The control parameters for these suspensions were kept the same as for their MR counterparts.

Half-vehicle model with rigid body

The steady-state and transient performance of the suspensions, relative to the passive one, for the rigid body vehicle is considered in this subsection.

Results for unevenness roads

The steady-state performance of the suspensions is assessed considering the disturbances induced by the movement of the vehicle, with constant velocity, on paved and asphalt roads. Figure 8 depicts the road induced disturbances at the front wheel for a vehicle speed $v = 20$ m/s and the following road parameters: paved road: $a = 0.45$ m^{-1} and $\sigma^2 = 3 \cdot 10^{-4}$ m^2; asphalt road: $a = 0.15$ m^{-1} and $\sigma^2 = 9 \cdot 10^{-6}$ m^2 (Hać, 1985).

In the results that follow, the steady-state performance of the suspensions was assessed in terms of root mean square (rms), maximum (max) and average deviation (d_{rms}) values. The average deviation d_{rms} of a signal is defined as the rms value of its time derivative and, therefore, it is supposed to provide more information about the frequency content of a signal than its rms value. The displacement and acceleration of point C (driver position, see Fig. 6); acceleration of point B (position of the seat-driver subsystem, Fig. 1) and deflections of the front suspension and tyre were considered in the analysis. The performance indices were computed for a simulation time $T = 10$ s.

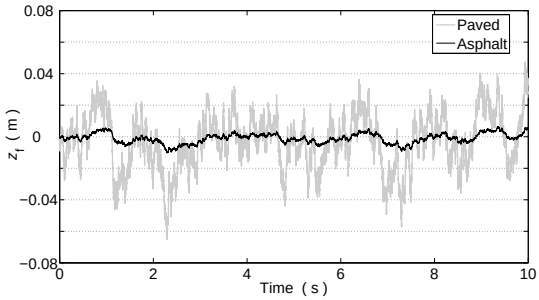

Figure 8. Steady-state disturbances at the front wheel for a vehicle speed $v = 20$ m/s.

Table 4. Relative performance of the suspensions for the rigid body vehicle and paved road.

		Suspension			
		LQG	VSC	MR-LQG	MR-VSC
q_C	rms	0.54	0.29	0.90	0.81
	max	0.52	0.30	0.89	0.87
	d_{rms}	0.47	0.35	0.88	0.79
$\ddot{q}_C$	rms	0.57	0.58	0.76	0.76
	max	0.58	0.59	0.68	0.67
	d_{rms}	0.72	0.71	0.70	0.70
$\ddot{q}_B$	rms	0.72	0.70	0.74	0.71
	max	0.70	0.67	0.66	0.69
	d_{rms}	0.77	0.70	0.74	0.74
$(q_{1f} - q_{2f})$	rms	1.06	1.06	1.14	1.14
	max	1.08	1.03	1.11	1.14
	d_{rms}	1.38	1.41	1.42	1.47
$(q_{2f} - z_f)$	rms	1.28	1.31	1.27	1.31
	max	1.08	1.12	1.03	1.08
	d_{rms}	1.03	1.03	1.03	1.03

The transient performance of the suspensions, on the other hand, was assessed considering the time responses of the acceleration at point B, which highlights the high frequency vibrations of the vehicle, since the seat acts as a filter to disturbances from point B to C.

The performance of the suspensions, relative to the passive one, for the rigid body vehicle and the disturbance induced by the paved road, is shown in Table 4. Considering the performance indices associated with the acceleration of points B and C, from Table 4, one can clearly note that all considered suspensions greatly improved on ride comfort, relative to the passive suspension. With respect to the acceleration of point B, the MR suspensions presented performances comparable to that of the active ones. The suspensions also improved on the performance indices associated with the displacement of point C, specially the VSC one, whose performance was greatly superior to that of the others suspensions. All considered suspensions presented relatively great d_{rms} values of suspension deflections, indicating a possibility of the presence of high frequency components in these signals. From Table 4, one may also observe that improvements on ride comfort were obtained at the expense of increasing tyre deflections.

For the rigid body vehicle traveling on the asphalt road with a speed $v = 20$ m/s, the considered suspensions also presented a great improvement on the ride comfort obtained by the standard passive suspension (Stutz, 2005). These results were omitted here.

Results for an impact bump

In order to assess the transient performance of the suspensions, the road-induced disturbance under the front wheel is assumed as

$$z_f(t) = \begin{cases} h_b \sin\left(\dfrac{\pi v(t-t_0)}{\omega_b}\right), & \text{for} \quad t_0 \le t \le t_0 + \dfrac{\omega_b}{v}; \\ 0, & \text{for} \quad t < t_0 \text{ or } t > t_0 + \dfrac{\omega_b}{v}, \end{cases} \tag{57}$$

where h_b and ω_b are, respectively, the height and width of the road irregularity, which has a sinusoidal profile with half wavelength, and t_0 is the initial time of the impact.

The road disturbance vector $\mathbf{z}$ is, therefore, obtained by considering that the rear disturbance is the time-delayed front one, viz.

$$z_r(t) = z_f\left(t - \frac{a_1 + a_2}{v}\right). \tag{58}$$

The transient disturbance induced by the movement of the vehicle, with constant velocity over an impact bump is depicted in Fig. 9. In this case, the disturbance parameters were adopted as: $h_b = 0.1$ m and $w_b = 0.5$ m.

As the LQG and MR-LQG suspensions require the knowledge of the road quality, described by parameter a, in the assessment of

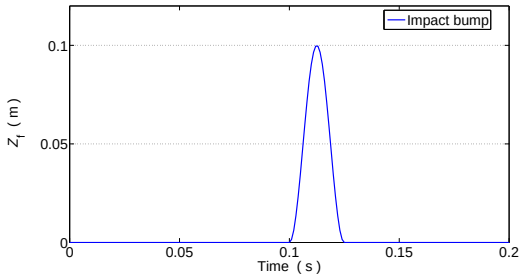

Figure 9. Transient disturbance at the front wheel for a vehicle speed $v = 20$ m/s.

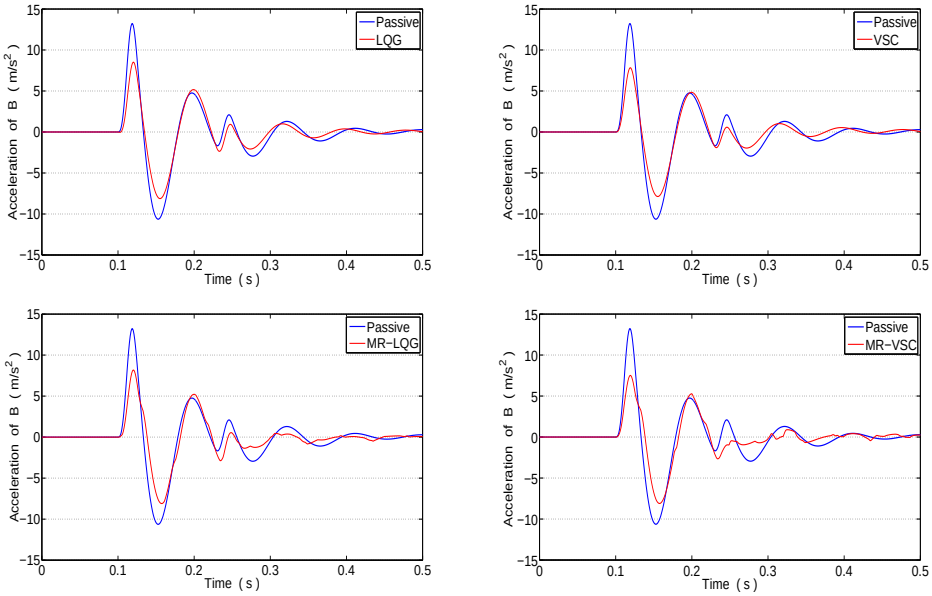

Figure 10. Acceleration of point B at the rigid body vehicle for the impact bump.

their transient performances, the value referent to the paved road was adopted.

The acceleration of point B for the rigid body vehicle travelling over the impact bump is depicted in Fig. 10. One may observe that all considered suspensions presented an improvement on the transient performance relative to that of the passive suspension, with significant reductions in the amplitude of the oscillations in some time intervals.

Half-vehicle model with flexible body

Despite not being considered for the synthesis of the suspensions, the flexibility of the vehicle body yields structural vibrations that may result in a great performance drop (Hać, Youn and Chen, 1996a; 1996b). This is due to the subjective discomfort from the direct exposure to high frequency vibrations or to noise derived from them. Hence, due to the control-structure interaction, accounting for the flexibility of the vehicle body in the performance assessment of the suspensions is a fundamental concern.

In order to take the flexibility of the vehicle body into account, the finite element method (Reddy, 1984) was considered. The vehicle body was modeled as an uniform beam and 10 Euler-Bernoulli beam elements, with 2 degrees of freedom per node, were used for its spatial discretization. Six elements were used for the discretization of the region between the suspensions and two elements were used for the discretization of each extreme region of the vehicle body (front and rear). The discretization was done in such a way that nodes of the finite element model were located at the connection points P_f and P_r between the suspensions and the vehicle body. The bending stiffness $EI = 1.53 \cdot 10^6$ Nm^2 was adopted for the vehicle body, so that its first bending natural frequency (17.21 Hz) fitted the corresponding one given by Hać et al. (1996a). It was also assumed a modal damping ratio $\zeta = 0.04$ for all bending modes of the structure. The other parameters of the model are as given in Tables 1 and 2.

The natural frequencies of the half-vehicle models with rigid body and flexible body, both considering the seat-driver subsystem, are shown in Table 5. Only the first three bending natural frequencies are shown.

According to Table 5, one may observe that the flexibility of the vehicle body yielded small changes in the first two natural frequencies of the system, associated with the translational and rotational modes of the vehicle body. The other natural frequencies presented no significant changes.

Results for unevenness roads

It is worth emphasizing that structural vibrations due to the flexibility of the vehicle body may present little increments on the rms values of acceleration signals, which are standard indices of ride comfort. Therefore, as the average deviation d_{rms} is supposed to provide more information about the frequency content of the signals, it will be used here as an important complementary index.

Table 6 presents the performance indices, associated with the ac-

Table 5. Natural frequencies of the vehicle models with rigid and flexible body.

Natural frequencies (Hz)	
Rigid Body	Flexible Body
1.06	1.01
1.31	1.22
3.93*	3.92*
8.06*	8.05*
11.63	11.63
11.79	11.79
22.58*	17.21
-	22.61*
-	47.46
-	93.06

* Natural frequencies associated with the seat-driver subsystem

Table 6. Relative performance indices for the passive suspension and paved road.

	rms	max	d_{rms}
$\ddot{q}_C$	0.99	1.00	1.09
$\ddot{q}_B$	1.05	1.05	1.72

Table 7. Relative performance of the suspensions for the flexible body vehicle and paved road.

		Suspension			
		LQG	VSC	MR-LQG	MR-VSC
q_C	rms	0.53	0.29	0.90	0.81
	max	0.53	0.31	0.95	0.91
	d_{rms}	0.46	0.34	0.89	0.79
$\ddot{q}_C$	rms	0.58	0.61	0.78	0.78
	max	0.59	0.60	0.68	0.65
	d_{rms}	0.72	0.73	0.72	0.74
$\ddot{q}_B$	rms	0.71	0.72	0.74	0.73
	max	0.68	0.67	0.79	0.78
	d_{rms}	1.02	0.54	0.93	0.96
$(q_{1f} - q_{2f})$	rms	0.97	0.93	1.12	1.09
	max	1.06	0.93	1.22	1.24
	d_{rms}	1.38	1.27	1.42	1.48
$(q_{2f} - z_f)$	rms	1.27	1.20	1.27	1.31
	max	1.07	1.05	1.03	1.12
	d_{rms}	1.03	1.02	1.03	1.03

celerations of points B and C due to the paved road, for the passive suspension and flexible body vehicle relative to the corresponding ones for the passive suspension and rigid body vehicle. From Table 6, one may observe that the rms and maximum values of the accelerations presented little or none influence of the vehicle body flexibility. On the other hand, due to the high frequency vibrations, the acceleration of point B at the flexible vehicle presented a considerably greater d_{rms} value. Since the seat acts as a filter to disturbances from point B to C, the acceleration of point C (driver position) presented no significant increase on the d_{rms} value.

Table 7 presents the performance of the suspensions, relative to the passive one, for the flexible body vehicle and the disturbance induced by the paved road. Although the flexibility of the vehicle body has not being considered for the synthesis of the suspensions, it can be seen that all suspensions greatly improved on ride quality. The performance indices associated with the acceleration of point C, along with the rms and maximum values of the acceleration of point B, were greatly improved. The suspensions also improved on the performance indices associated with the displacement of point C. The active suspensions presented greater improvements on these last indices, specially the VSC one, whose performance, as in the rigid body case, was greatly superior to that of the others suspensions. It is worth noting that the MR suspensions presented maximum values of the front suspension deflections significantly greater than that of the passive suspension. All suspensions presented relatively great d_{rms} values of deflections.

Table 8. Relative performance of the suspensions for the flexible body vehicle and the asphalt road.

		Suspension			
		LQG	VSC	MR-LQG	MR-VSC
q_C	rms	0.61	0.30	0.80	0.75
	max	0.58	0.30	0.82	0.79
	d_{rms}	0.49	0.31	0.74	0.65
$\ddot{q}_C$	rms	0.54	0.53	0.74	0.77
	max	0.58	0.50	0.69	0.65
	d_{rms}	0.71	0.73	1.05	1.25
$\ddot{q}_B$	rms	0.69	0.68	0.88	1.00
	max	0.69	0.61	0.93	1.12
	d_{rms}	0.98	0.55	1.95	2.25
$(q_{1f} - q_{2f})$	rms	0.94	1.02	0.94	0.87
	max	0.92	1.07	1.00	0.96
	d_{rms}	1.36	1.25	1.30	1.17
$(q_{2f} - z_f)$	rms	1.25	1.18	1.18	1.08
	max	1.11	1.07	1.08	1.09
	d_{rms}	1.03	1.02	1.02	1.01

The performance of the suspensions, relative to the passive one, for the flexible body vehicle and the disturbance induced by the asphalt road is given in Table 8. From the presented results, it can be clearly seen that the active suspensions greatly improved on ride comfort. The MR suspensions, on the other hand, presented great improvements only on the rms and maximum values of the acceleration of point C (driver position). With respect to the acceleration of point B, only the MR-LQG presented an improvement on the rms and maximum values. However, it must be emphasized here that the road induced disturbances are assumed to be known in the LQG and MR-LQG suspensions, which yields higher performances than in a practical application. The MR suspensions presented higher d_{rms} values of the acceleration of points B and C, especially the MR-VSC. All considered suspensions improved on the performance indices associated with the displacement of point C.

Results for an impact bump

The influence of the vehicle body flexibility on the transient performance of the suspensions is depicted in Fig. 11. The acceleration of point B, due to the impact bump shown in Fig. 9, at the rigid and flexible vehicles with passive, active and MR suspensions is considered. From Fig. 11, one can clearly note the influence of the body flexibility on the amplitude of the oscillations and on the presence of high frequency components in the acceleration of point B at the flexible vehicle. The MR suspensions presented greater performance drops, due to the flexibility of the vehicle body, than the active ones. It is worth noting that although the VSC suspension was able to quickly suppress the high frequency vibrations in the acceleration of point B, in the MR-VSC suspension, the high frequency vibrations lasted for longer times and presented higher amplitudes.

Due to their semi-active nature, the MR dampers are not able to reproduce the desired control force, but only an approximate one. In order to illustrate this fact, Fig. 12 depicts the desired control force, resulted from the variable structure control approach, Eqs. (33)-(35), and the actual force provided by the MR damper, along with the corresponding input voltage yielded by the clipped-control algorithm, Eq. (38). Only the transient responses associated with the front MR damper in the MR-VSC suspension were considered. The acceleration of point B is also depicted. From Fig. 12, one may observe that the amplitude of the high frequency vibrations in the acceleration of B is greater within the intervals where the input voltage assumes its maximum value (2V) for long and at the end of the depicted time interval, where a high frequency content may be observed in the applied control force.

From the results presented, one can clearly note a drop in the performance of the suspensions due to the flexibility of the vehicle body. Greater performance drops were presented by the MR suspensions, mainly for the asphalt road and the impact bump. However, in these suspensions, a high frequency control action may result from the clipped-control algorithm, which was used to select the input voltage to the MR dampers between the extreme values 0 and $V_{max} = 2$ V. Besides, if the road-induced disturbances are not sufficient to yield the MR fluid through the damper valves, the dampers will behave as rigid elements between the vehicle body and the wheels. Then, in these cases, all vibration energy will be transmitted to the vehicle body by the suspension system. Therefore, MR dampers with lower yield strengths may result in greater improvements on ride comfort, mainly in the asphalt road and impact bump disturbances.

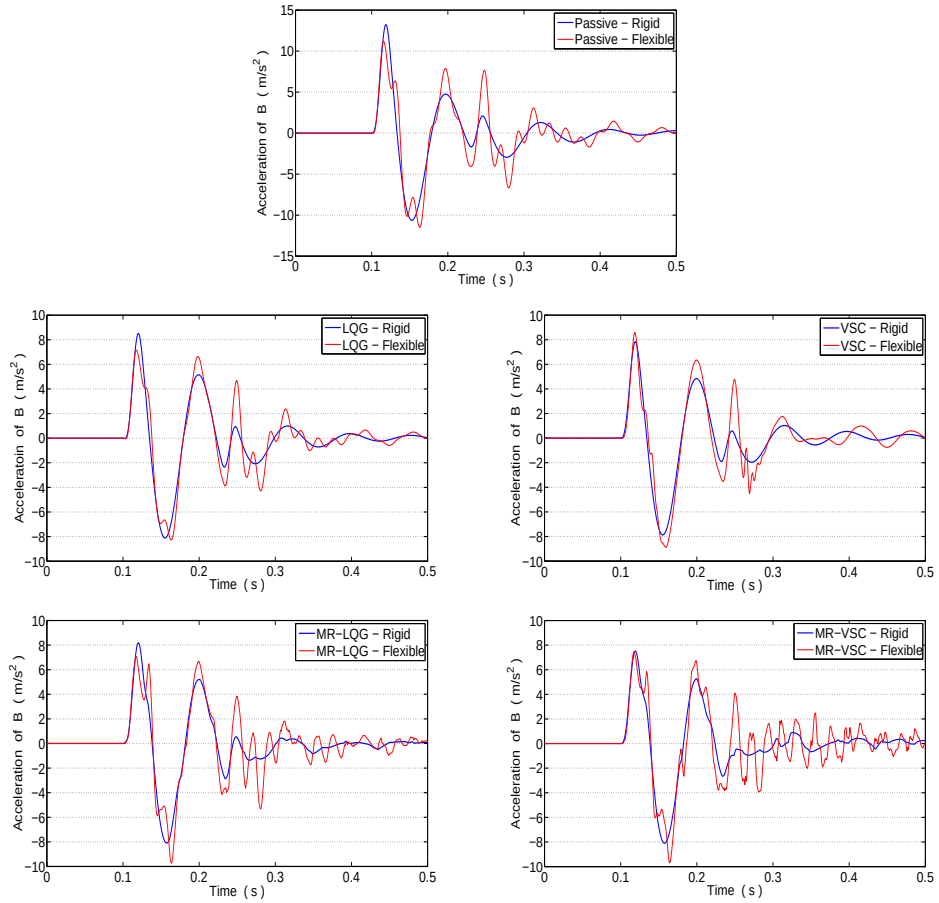

Figure 11. Acceleration of point B at the rigid and flexible vehicles for the impact bump.

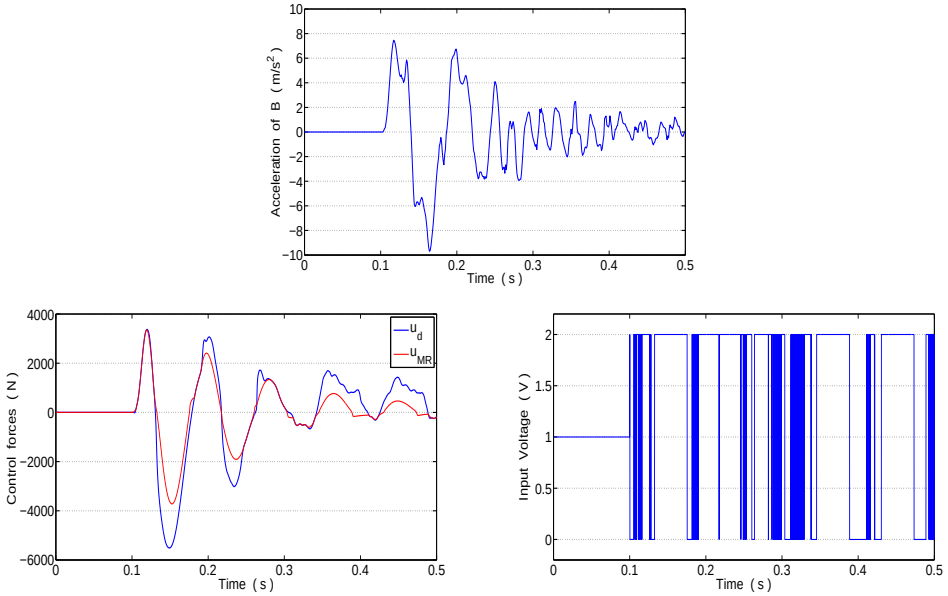

Figure 12. Transient responses associated with the MR-VSC suspension.

Acknowledgements

The authors gratefully acknowledge the Brazilian National Council for Scientific and Technological Development (CNPq) and Rio de Janeiro's Foundation for Research Support (FAPERJ) for their financial support to this research.

References

Anderson, B.D.O. and Moore, J.B., 1990, "Optimal Control: Linear Quadratic Methods", Prentice-Hall.

Carlson, J.D. and Spencer Jr., B.F., 1996, "Magneto-Rheological Fluid Dampers: Scalability and Design Issues for Application to Dynamic Hazard Mitigation", Proceedings of the 2nd International Workshop on Structural Control, Hong Kong, pp. 99-109.

Chang, C.C. and Zhou, L., 2002, "Neural Network Emulation of Inverse Dynamics for a Magnetorheological Damper", *Journal of Structural Engineering*, Vol. 128, No. 2, pp. 231-239.

Choi, S.B., Lee, S.K. and Park, Y.P., 2001, "A Hysteresis Model for the Field-dependent Damping Force of a Magnetorheological Damper", *Journal of Sound and Vibration*, Vol. 245, No. 2, pp. 375-383.

Du, H., Sze, K.Y. and Lam, J., 2005, "Semi-Active H_∞ control of Vehicle Suspension with Magneto-Rheological Dampers", *Journal of Sound and Vibration*, Vol. 283, pp. 981-996.

Edwards, C. and Spurgeon, S.K., 1998, "Sliding Mode Control: Theory and Applications", Francis & Taylor Ltd.

Hać, A., 1985, "Suspension Optimization of a 2-DOF Vehicle Model using a Stochastic Optimal Control Technique", *Journal of Vibration and Control*, Vol. 100, No. 3, pp. 343-357.

Hać, A., Youn, I. and Chen, H.H., 1996a, "Control of Suspensions for Vehicles with Flexible Bodies - Part I: Active Suspensions", *Trans. of The ASME, Journal of Dynamic Systems, Measurement and Control*, Vol. 118, pp. 508-517.

Hać, A., Youn, I. and Chen, H.H., 1996b, "Control of Suspensions for Vehicles with Flexible Bodies - Part II: Semi-Active Suspensions", *Trans. of The ASME, Journal of Dynamic Systems, Measurement and Control*, Vol. 118, pp. 518-525.

Hrovat, D., 1997, "Survey of Advanced Suspension Developments and Related Optimal Control Applications", *Automatica*, Vol. 33, No. 10, pp. 1781-1817.

Jansen, L.M. and Dyke, S.J., 2000, "Semi-Active Control Strategies for MR Dampers: A Comparative Study", *ASCE Journal of Engineering Mechanics*, Vol. 126, No. 8, pp. 795-803.

Lai, C.Y. and Liao, W.H., 2002, "Vibration Control of a Suspension System via a Magnetorheological Fluid Damper", *Journal of Sound and Vibration*, Vol. 8, pp. 527-547.

Liangbin, C. and Dayue, C., 2004, "Two-Stage Vibration Isolation System Featuring an Electrorheological Damper via the Semi-Active Static Output Feedback Variable Structure Control Method", *Journal of Vibration and Control*, Vol. 10, pp. 683-706.

Marzbanrad, J., Ahmadi, G., Hojjat, Y. and Zohoor, H., 2002, "Optimal Active Control of Vehicle Suspensions System Including Time Delay and Preview for Rough Roads", *Journal of Vibration and Control*, Vol. 8, pp. 967-991.

Nguyen, Q.H. and Choi, S.B., 2009, "Optimal Design of MR Shock Absorber and Application to Vehicle Suspension", *Smart Materials and Structures*, Vol. 18, pp. 1-11.

Reddy, J.N., 1984, "An Introduction to the Finite Element Method", McGraw-Hill Book Company.

Roh, H.S. and Park, Y., 1999, "Stochastic Optimal Preview Control of an Active Vehicle Suspension", *Journal of Sound and Vibration*, Vol. 220, No. 2, pp. 313-330.

Sharp, R.S. and Hassan, S.A., 1986, "An Evaluation of Passive Automotive Suspension Systems with Variable Stiffness and Damping Parameters", *Vehicle System Dynamics*, Vol. 15, pp. 335-350.

Shirahatt, A., Prasad, P.S.S., Panzade, P. and Kulkarni, M.M., 2008, "Optimal Design of Passenger Car Suspension for Ride and Road Holding", *Journal of the Brazilian Society of Mechanical Sciences and Engineering*, No. 1, pp. 66-76.

Smith, C.C., McGehee, D.Y. and Healey, A.J., 1978, "The Prediction of Passenger Riding Comfort from Acceleration Data", *ASME J. Dynamic Systems, Measurement and Control*, Vol. 100, pp. 34-41.

Spencer Jr., B.F., Dyke, S.J., Sain, M.K. and Carlson, J.D., 1996, "Phenomenological Model of a Magneto-Rheological Damper", *ASCE, Journal of Engineering Mechanics*, Vol. 123, No. 3, pp. 230-238.

Stutz, L.T., 2005, "Synthesis and Analysis of a Magneto-Rheological Suspension Based on the Variable Structure Control Approach", Doctoral Thesis, Federal University of Rio de Janeiro, Rio de Janeiro, Brazil.

Stutz, L.T. and Rochinha, F.A., 2005, "A Comparison of Control Strategies for Magnetorheological Vehicle Suspension Systems", Proceedings of the XII International Symposium on Dynamic Problems of Mechanics, Brazil.

Stutz, L.T. and Rochinha, F.A., 2007, "Magneto-Rheological Vehicle Suspension System based on the Variable Structure Control applied to a Flexible Half-Vehicle Model", Proceedings of the XII International Symposium on Dynamic Problems of Mechanics, Brazil.

Sung, K.G., Han, Y-M., Cho, J-W. and Choi, S-B., 2008, "Vibration control of vehicle ER suspension system using fuzzy moving sliding mode controller", *Journal of Sound and Vibration*, Vol. 311, pp. 1004-1019.

Wei, L. and Griffin, M.J., 1998a, "Mathematical Models for the Apparent Mass of Seated Human Body Exposed to Vertical Vibration", *Journal of Sound and Vibration*, Vol. 212, No. 5, pp. 855-874.

Wei, L. and Griffin, M.J., 1998b, "The Prediction of Seat Transmissibility from Measures of Seat Impedance", *Journal of Sound and Vibration*, Vol. 214, No. 1, pp. 121-137.

Yokoyama, M., Hedrick, J.K. and Toyama, S., 2001,"A Model Following Sliding Mode Controller for Semi-Active Suspension Systems with MR Dampers", Proceedings of the American Control Conference, Arlington, pp. 2652-2657.

Yoshimura, T., Kume, A., Kurimoto, M. and Hino, J., 2001, "Construction of an Active Suspension System of a Quarter Car Model using the Concept of Sliding Mode Control", *Journal of Sound and Vibration*, Vol. 139, No. 2, pp. 187-199.